Microchimica Acta (2020) 187: 214
https://doi.org/10.1007/s00604-020-4184-0

ORIGINAL PAPER

A gold nanoparticle-based colorimetric mercury(II) biosensor using a DNA probe with phosphorothioate RNA modification and exonuclease III-assisted signal amplification

Yunpeng Xing [1,2,3] · Qian Zhu [1] · Xiaohong Zhou [1,3] · Peishi Qi [2]

Received: 20 September 2019 / Accepted: 24 February 2020 / Published online: 11 March 2020

Abstract

Herein, we report a rapid and sensitive colorimetric detection of Hg^{2+} by designing a specific DNA probe with phosphorothioate RNA modification (PS-probe) for Hg^{2+} recognition and utilizing DNA-modified gold nanoparticles (DNA-AuNPs) as the transducer. The distance between two DNA-AuNPs is controlled by a linker DNA, providing the linker DNA-regulated aggregation or dispersion status of AuNPs in solution. Exonuclease III (Exo III) can trigger the recycled digestion of linker DNA strands, inhibiting the reformation of aggregated nanoparticles and hence leading to a color shift from purple to red. However, the Hg^{2+}-induced cleavage of the PS-probe can efficiently prevent the digestion of linker DNA strands by Exo III and hence reassemble the modified AuNPs to form aggregates in purple color. Thus, a positive correlation between the linker DNA strands left and the addition of Hg^{2+} provides a quantitative basis for Hg^{2+} sensing. A linear range of A_{520}/A_{700} versus Hg^{2+} concentration is achieved in the range 2–100 nM associated with a detection limit as low as 1.30 ± 0.04 nM. Moreover, the biosensor exhibits excellent selectivity for Hg^{2+}. The strong selectivity behavior was confirmed by recoveries ranging from 96 to 114% in real water samples.

Keywords Trace Hg(II) ions · Phosphorothioate-modified RNA · Colorimetric biosensor · Environmental water samples

Introduction

Mercury is generally considered to be one of the most toxic metals found in nature, which is mainly released from mercury-related industries [1]. Considering its bioaccumulation characteristics, the severe adverse health effect of mercury on human beings cannot be overlooked even at trace concentration level [2]. While the traditional instrumental techniques, for example, inductively coupled plasma mass spectrometry (ICP-MS), are accurate and widely used for mercury detection, their applications are still limited to the laboratory due to the expensive and large-scale equipment and complicated detection procedure. Therefore, developing facile and sensitive detection methods of mercury in the environments is still of great importance. Considering the divalent mercury (Hg^{2+} ions) are water-soluble and one of the most common and stable existing form in water environments among the mercury pollution [3], the development of novel Hg^{2+} detection has been focused and received a lot of attentions.

To meet the goals of facile and sensitive analysis, the biosensor technique emerges as an effective alternative to the traditional analytical techniques. By virtue of their high sensitivity, specificity, and facile synthesis, functional nucleic acid (FNA)-based biosensors have received numerous attentions and witnessed their broad applications ranging from environmental monitoring [4], diagnostics [5],

Yunpeng Xing and Qian Zhu contributed equally to this work.

Electronic supplementary material The online version of this article (https://doi.org/10.1007/s00604-020-4184-0) contains supplementary material, which is available to authorized users.

✉ Xiaohong Zhou
xhzhou@mail.tsinghua.edu.cn

✉ Peishi Qi
qipeishi@163.com

[1] State Key Joint Laboratory of ESPC, School of Environment, Tsinghua University, Beijing 100084, China

[2] State Key Laboratory of Urban Water Resource and Environment, School of Environment, Harbin Institute of Technology, Harbin 150090, China

[3] National Engineering Laboratory for advanced technology and equipment of water environment pollution monitoring, Changsha 410205, China

and food safety to basic research [6]. Since Hg^{2+} was reported to be specifically bound between two thymine bases, thus promoting the T-T mismatch [7], various T-Hg^{2+}-T interaction-based biosensors for Hg^{2+} detection were reported with different transduction modes used, including electrochemistry [8], colorimetry [3], surface plasmon resonance [9], fluorescence [10], and surface-enhanced Raman scattering [11]. Although these biosensors need less professional personnel and simpler sensing instrument than traditional methods, the Hg^{2+}-driven T-T mismatch was reported to be strongly affected by reaction buffer conditions, including pH, temperature, ionic strength, and ion species [12–14]. DNAzyme is used as another DNA-based strategy for sensing Hg^{2+} [15, 16]. While Hg^{2+} can activate some catalysis of DNAzymes, the high detection limits and low catalytic efficiency limited their downstream applications [10]. Although some DNAzymes have been reported with high sensitivity, the T-Hg^{2+}-T interaction has to be incorporated in the design of such DNAzyme [17], which makes the sensing system very complicated. Recently, a new strategy for specific Hg^{2+} sensing was reported by using a specifically designed DNA probe, which incorporated phosphorothioate (PS)-modified RNA linkages [18]. This DNA probe inserted with PS-modified RNA can efficiently and specifically cleaved by Hg^{2+} ions due to their strong thiophilicity. Considering that the cleavage procedure is a chemical reaction, this sensing strategy was reported to be less affected by the reaction conditions and show excellent selectivity [12, 18].

Colorimetric biosensors, especially by using the gold nanoparticles (AuNPs) as indicators, have been extensively utilized due to its simplicity of operation and visibility of observation [19]. The peak of the absorption spectra of AuNPs is dependent on their size and shape, providing a quantitative basis for colorimetric sensing. Compared with the unmodified AuNPs (in the general sense, citrate-stablized AuNPs), DNA-modified AuNPs (DNA-AuNPs) by using thiol-gold chemistry can provide harsher environment resistance and higher reliability, which have been developed and utilized in detecting different targets, such as DNA sequence [20], metal ions [21], and bacteria [22].

Stated thus, by merging the virtues of the DNA probe inserted with PS-modified RNA for Hg^{2+}-specific recognition, Exo III-assisted signal amplification, and DNA-AuNPs as stable indicators of colorimetry, we herein develop a visible, cost-effective, easy-to-handle yet sensitive biosensor for the colorimetric detection of Hg^{2+} in aqueous environments. As a result, the specificity provided by the DNA probe inserted with PS-modified RNA towards Hg^{2+} is exclusive; moreover, the limit of detection can reach 1.30 nM via the color variance of AuNPs, which allows the turnaround time after sample collection from suspicious sites to be limited to 40 min.

Methods

Preparation of DNA probes The list of chemicals used is described in Electronic Supplementary Material (ESM). The stock solution of different DNA probes was prepared by using 10-mM HEPES buffer (pH 7.5) to dissolve the oligonucleotides to 10 μM strand concentration. The solution was heated at 95 °C for 5 min and then gradually cooled to room temperature in 2 h. All stock solutions were maintained at 4 °C before the use. If not specified, all buffers used in this work were prepared either in biomolecule grade deionized water or DEPC-treated deionized water (in general referring to DI water).

Preparation and modification of AuNPs AuNPs in diameter of 13 nm were prepared by reducing $HAuCl_4$ using sodium citrate [23]. Briefly speaking, 100 mL of 1 mM $HAuCl_4$ was heated to reflux under the condition of stirring, and subsequently, 10 mL of 38.8 mM sodium citrate was added. The color of mixture changed from light yellow to heavy red within a few minutes. After that, the mixture was left to reflux for another half hour, completing the reduction of $HAuCl_4$ to gold nanoparticles. The morphology of AuNPs was characterized using TEM (Fig. S1), and their average size was determined to be approximately 12 ± 2 nm by counting more than 100 particles from TEM pictures.

The functionalization of AuNPs with 3′- or 5′-thiol-modified DNA strands followed the previously reported procedures [24]. Briefly speaking, 90 μL of 100 μM DNA1 or DNA2 was activated by tris(2-carboxyethyl)phosphine hydrochloride (TCEP) for 1 h. Subsequently, 3 mL AuNPs was added into the mixture and incubated for 16 h. After that, 31 μL of 500 mM sodium acetate was then added drop by drop and incubated for another 24 h. After centrifugation, the supernatant was discarded, and 1.2 mL buffer containing 25 mM Tris-acetate and 100 mM NaCl (pH 8.2) was then added. After centrifugation again, the supernatant was removed, and the DNA-modified AuNPs were dispersed in 3 mL buffer (25 mM Tris-Acetate and 300 mM NaCl, pH 8.2).

Nondenaturing PAGE For a typical nondenaturing PAGE, the DNA samples were diluted by using 6 x loading buffer with a volume ratio of 5:1. The 15% polyacrylamide (19:1 acrylamide/bisacrylamide) gels were freshly prepared. The nondenaturing PAGE were performed in 1 x TBE under the conditions of 80 V, 50 min, and 20 °C. Gels were stained with GelRed Acid Gel Stain and imaged under UV exposure by FLS-5100 film (Fuji, Japan). The measurements were performed in 10 mM HEPES buffer (pH 7.5).

Absorbance measurement Under the optimized conditions (see Fig. S2), the absorbance measurement methods towards Hg^{2+} were developed. A series of Hg^{2+} standard solutions

(0.3, 1.5, 3.0, 4.5, 7.5, 11.25, 15, and 30 μM) was prepared by diluting the stock solution of Hg^{2+} with DI water. 10 μM strand concentration of probes and linker were prepared by diluting the DNA stock solutions, respectively, with 10 mM HEPES buffer (pH 7.5). The optimal steps for Hg^{2+} detection were listed as follows: 1 μL Hg^{2+} standard solution under various concentrations was successively added into 4 μL of 150 nM PS-probe for incubation of 15 min. Subsequently, 1 μL 150 mM Mg^{2+} solution, 2 μL purified water, 1 μL 10 μM linker strand, and 5 U Exo III were added to the solution described above to catalyze the hydrolysis reaction for another incubation of 30 min at 37 °C. The reaction mixture was then heated to 65 °C for 10 min to stop the digestion reaction by inactivating the Exo III activities. Finally, 20 μL DNA1-Au, 20 μL DNA2-Au, and 100 μL of 15 mM HEPES buffer (pH 7.5) were added for final incubation of 10 min before the absorbance measurements. The Hg^{2+} concentrations in the samples were 2, 10, 20, 30, 50, 75, 100, and 200 nM, respectively. The optical chamber (1-cm path length, 0.35-mL volume) was used for absorbance measurements in the wavelength range of 400 to 750 nm at room temperature (approximately 25 °C).

Selectivity and recovery The selectivity of this method was tested using Mn^{2+}, Pb^{2+}, Ca^{2+}, Cd^{2+}, Cu^{2+}, Ni^{2+}, Fe^{2+}, Cr^{3+}, and Co^{2+} (each at 100 nM) in the presence or absence of 10 nM Hg^{2+}, respectively. The absorption ratios of A_{520}/A_{700} for competing species were recorded. Furthermore, the metal ions described above were incubated with the PS-probe (1 μM) for 10 min. The product after incubation was separated on 15% nondenaturing PAGE gels and analyzed by using a FLS-5100 film imaging system.

Environmental water samples were taken from Guanting reservoir (Beijing, China) to test the reliability of this method. Sample solutions were taken and then passed through a 0.2-μm pore-size membrane filter before test. Subsequently, the water samples were spiked with various Hg^{2+} to final concentrations of three levels (0, 5, and 10 nM). Detection procedures were performed based on the optimal conditions for Hg^{2+} detection described above.

Results and discussion

Working principle Figure 1 illustrates the principle scheme of colorimetric biosensing of Hg^{2+} using a DNA probe inserted with phosphorothioate-modified RNA and Exo III-assisted signal amplification. The colorimetric determination system comprises a PS-probe, a linker strand of DNA, Exo III, and two sets of different DNA-AuNPs (called DNA1-Au and DNA2-Au, respectively) with sequences complementary to both ends of the linker strand of DNA, respectively. It should be noted that the linker DNA strand is rationally designed in such a way that, if Hg^{2+} is absent, the linker will hybridize with the PS-probe to form a specific duplex with a recessed 3′ terminal end, which can be cleaved by Exo III. Considering that Exo III can only digest the 3′ recessed single-stranded DNA of linker strand, the PS-probe will hence be recycled to hybridize more linker strands to undergo new digestion reactions. Such an Exo III-assisted cyclic hybridization-hydrolysis process may trigger the digestion of numerous linker DNA strands, resulting in a significantly amplified signal transduction. By contrast, the presence of Hg^{2+} ions can efficiently cleave the phosphorothioate RNA linkage incorporated in the PS-probe due to their extremely strong thiophilicity [18]. This will prevent the digestion of linker strands by the enzyme of Exo III. Upon completion of the digestion/cleavage cycle, the mixtures of DNA1-Au and DNA2-Au are added into the solution. As a result of the complementary hybridization of DNA1-Au and DNA2-Au to both ends of the linker DNA strand, a color change of AuNPs from red to purple would be obtained by shortening their distance between DNA1-Au and DNA2-Au and used to quantify the amount of the remaining linker DNA strands. Considering a positive correlation between the linker strand left and the addition of Hg^{2+}, Hg^{2+} concentration can be quantified accordingly.

The UV–vis spectra of colorimetric modified-AuNP system in the presence of different Hg^{2+} concentrations are shown in Fig. 2a. Initially, the linker strand complementary to the 12-mer DNAs on AuNPs assembled the nanoparticles closer to form purple-colored aggregates, exhibiting the plasmon resonance absorption at about 600 nm (curve *a*). Meanwhile, the linker hybridized with PS-probe strand to form a 3′ terminus end recessed duplex that was digestible by Exo III. Due to the function of Exo III, the 3′ recessed linker strand was cleaved into single bases, which was not able to assemble the modified AuNPs of DNA1-Au and DNA2-Au. The dispersed AuNPs were accompanied with a plasmon resonance absorption peak at about 520 nm (curve *b*). However, following the addition of 200 nM Hg^{2+}, the absorbance of AuNPs decreased significantly at 520 nm and increased in a longer wavelength range with a peak value at approximately 600 nm, resulting into the red-to-purple color shift (curve *c*). It was attributed to the Hg^{2+}-triggered cleavage of PS-probe, which ended the cyclic Exo III enzymatic amplification. By contrast, the DNA sequence without phosphorothioate-modified RNA linkage (WPS-probe) was designed, and its responses towards Hg^{2+} were investigated for comparison. As shown in curve *d*, the absorbance spectra had a slight change when 200 nM Hg^{2+} were incubated with WPS-probe compared to the sensing system without Hg^{2+} (curve *a*). Inset of Fig. 2a shows the photos under four conditions, accordingly. The colorimetric visualization with the naked eye was achieved without using the complicated instrumentation. These results concurred with our speculation that

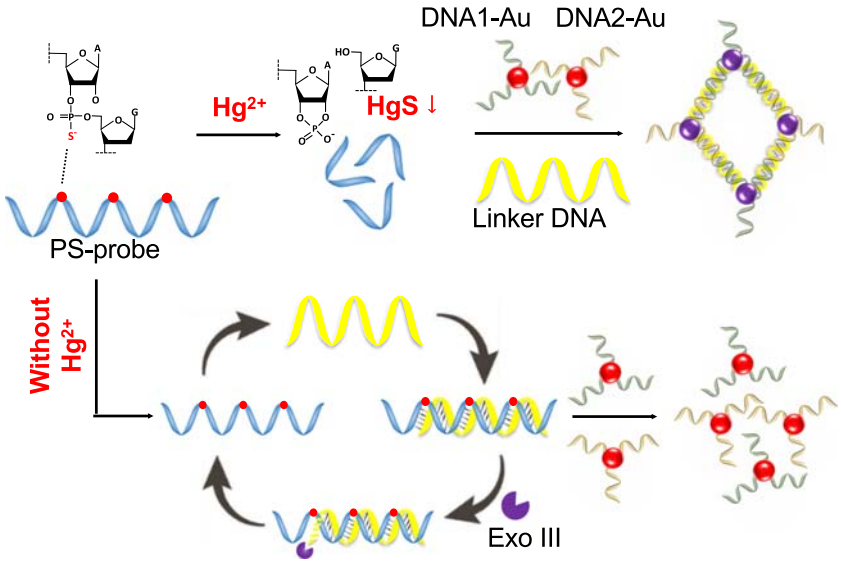

Fig. 1 Sensing mechanism of Hg^{2+} using a DNA probe with phosphorothioate RNA modification (PS-probe) and Exo III-assisted signal amplification. Two sets of AuNPs modified with DNA sequences complementary to each end of the linker DNA strand, respectively, are represented by DNA1-Au and DNA2-Au

Hg^{2+} trigger the cleavage of the phosphorothioate-modified RNA linkage rather than unmodified one and hence change the aggregation status of AuNPs. Meanwhile, the phenomena described above accorded well with numerous previous studies [22].

The changes in the aggregation status of DNA1-Au and DNA2-Au nanoparticles in the Exo III amplification system were verified by the TEM technique. As illustrated in Fig. 2b, DNA-AuNPs were well dispersed with no addition of Hg^{2+} due to the effective Exo III-assisted digestion of the linker strand in a duplex form with PS-probe (*Left*). However, upon adding Hg^{2+}, two sets of DNA-AuNPs were assembled by the linker strands considering that their digestion was apparently inhibited due to the significant cleavage ability of Hg^{2+} on the PS-probe (*Right*). In addition, the nondenaturing PAGE was used to characterize the cleavage process of PS-probe induced by Hg^{2+} ions. Figure 2c demonstrates the images of nondenaturing PAGE for PS-probe in 10 mM HEPES buffer (pH 7.5) at room temperature. We observed three distinct bands with unequal mobilities in the PS-probe system, implying the DNA sequences with different lengths formed. The faster two bands exhibited that the PS-probe underwent cleavage, while an increase in the cleaved fraction was found when more Hg^{2+} existed. This result confirmed that the existence of

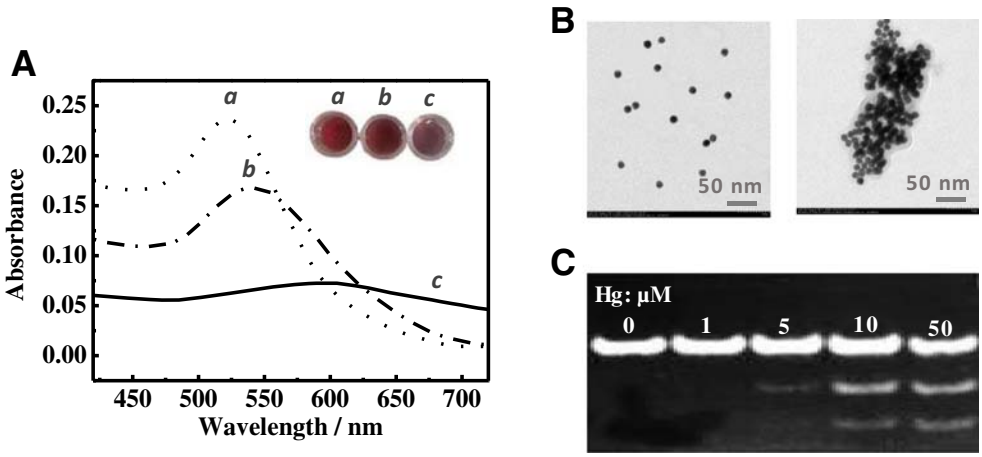

Fig. 2 **a** Absorption spectra of the modified AuNP system in the presence of (a) linker strand; (b) linker strand, PS-probe, and Exo III; (c) linker strand, PS-probe, and Exo III after incubation with Hg^{2+}; and (d) linker strand, WPS-probe, and Exo III after incubation with Hg^{2+}. DNA1-Au, 3.2 nM; DNA2-Au, 3.4 nM; linker, 67 nM; PS-probe, 4 nM; WPS-probe, 4 nM; Exo III 5 units (U); Hg^{2+}, 200 nM; and pH 7.5. Inset shows the photos under four conditions, accordingly. **b** TEM images of AuNPs containing PS-probe. DNA1-Au, 3.2 nM; DNA2-Au, 3.4 nM; linker, 67 nM; PS-probe, 4 nM; Exo III 5 U; pH 7.5; and Hg^{2+}, 0 (*Left*) and 200 nM (*Right*). **c** Nondenaturing 15% PAGE image (lane 1 to lane 5 from left to right) exhibiting the cleavage products of PS-probe incubated with 0, 1, 5, 10, and 50 μM Hg^{2+}, respectively, for 10 min

Hg^{2+} can induce the cleavage of PS-probe. The DNA sequence at the slowest band was explained to its desulfurization to the normal phosphate backbone and was not cleaved by Hg^{2+}again [12]. The cleavage yield that has yet to be optimized may also contribute to this phenomenon [25].

Optimization of bioassay conditions Optimization processes were conducted to identify the optimal bioassay conditions of this colorimetric method for Hg^{2+} detection. Three key factors for the modified AuNPs-based colorimetric bioassay as suggested by previous studies [3, 26, 27], including the linker concentration, the magnesium ion concentration in buffer, and the Exo III concentration, were investigated. The linker concentration should have a great impact on the colorimetric biosensing because of it being responsible for the assembly of DNA1-Au and DNA2-Au nanoparticles. Unveiled by Fig. S2A, the higher linker concentrations resulted in greater color changes represented in the form of ration of absorption intensity A_{520}/A_{700}, however reached relatively steady when the linker concentration was higher than 20 nM. To increase the detection sensitivity, 20 nM linker strand was chosen for the subsequent experiments. The magnesium ion salt was added to enhance the linker DNA-induced nanoparticle assemblies, and therefore, the concentration of Mg^{2+} on the performance was exploited. Unveiled by Fig. S2B, no significantly observable change in A_{520}/A_{700} was obtained until 1 mM Mg^{2+} ions; however, the value decreased sharply when the Mg^{2+} concentrations further increased. To obtain a better sensitivity in the color change, 1 mM Mg^{2+} was used in the following experiments. In the end, the influence of the Exo III concentration was investigated as illustrated in Fig. S2C. Under the condition of Exo III concentration below 5 U, A_{520}/A_{700} changes with the enzyme concentration showed opposite trends in the absence (R1) and presence (R2) of target. However, R1 and R2 values reached steady with increased Exo III concentration under both conditions. The highest ratio R1 to R2 was 2.1, at which the concentration of Exo III was 5 U, so we selected 5 U Exo III, 20 nM linker strand, and 1 mM Mg^{2+} as the optimal detection conditions.

Moreover, the number of PS-modified RNA linkage has a great impact on the cleavage reaction yield [28]. The DNA sequence inserted with two, three, and four PS-modified RNA linkages (referring to PS2-probe, PS3-probe, and PS4-probe) were tested by incubating in the absence or presence of 100 nM Hg^{2+}, respectively, under optimal conditions. The A_{520}/A_{700} values are demonstrated in Fig. S2D. As we expected, the increase in the number of PS-modified RNA linkages resulted in more significant signal changes, indicating the greater cleavage reaction yield. Three and four PS-modified RNA linkages exhibited a slight difference to increase the cleavage performance. Compromising the cleavage capability and the price of the probe synthesis, the PS-probe with three PS-modified RNA linkage was chosen for the experiments.

Performance for Hg^{2+} determination Under the optimal bioassay conditions, the sensitivity of this colorimetric sensing system for Hg^{2+} determination was evaluated. The visible spectra of modified AuNPs under different Hg^{2+} concentrations are demonstrated in Fig. 3a. Initially, this modified AuNPs (DNA1-Au, DNA2-Au) with modification of non-complimentary DNA sequences as the stabilizer [29] exhibited red in color, accompanied by a strong plasmon resonance absorption at about 520 nm (curve 1) due to the Exo III-assisted recycling of digesting the linker DNA strand via its hybridization with PS-probe. However, the existence of Hg^{2+} would cleave PS-probe into short fragments, which inhibited its hybridization with the linker DNA and hence avoided its digestion by Exo III. As a result, the remaining linkers would assemble the DNA1-Au and DNA2-Au nanoparticles closer, enabling AuNPs aggregated. Theoretically, the AuNPs aggregated quicker with the increased Hg^{2+} concentration, therefore leading to more aggregated AuNPs in a certain period of time. Following the addition of Hg^{2+}, curves 2–9 displayed an observable decrease in the peak of absorption at 520 nm, accompanied by an increase in the longer wavelength range with a peak value at 600 nm. This result corresponded to a red-to-purple color change (Inset of Fig. 3a).

We compared the sensitivity by means of the signal represented by the ratios of absorbance intensities, A_{520}/A_{700} and A_{520}/A_{600}, respectively. The linear relationship between A_{520}/A_{700} values and different Hg^{2+} concentration is represented in Fig. 3b. The linear regression range exhibited 2–100 nM Hg^{2+} ($R^2 = 0.99$) and a limit of determination (LOD) of 1.30 nM using the three-sigma method [30]. It is indicated that A_{520}/A_{700} is more sensitive than A_{520}/A_{600} to the change of Hg^{2+} concentration (Fig. S3) although their linear fitting results with Hg^{2+} concentration shared a same linear range (see Table S2).

Nanomaterials especially Au and Ag in the form of nanoparticles and nanorods are widely used in designing colorimetric strategies for Hg^{2+} determination; however, these colorimetric assays often suffered from low sensitivity [26]. A comparison of the analytical performance of this work with those obtained by several other approaches based on for the determination of Hg^{2+} is shown in Table 1**.** Obviously, the LOD of our method was comparable with most of the reported Hg^{2+} biosensing techniques. In our system, such an attractive LOD was mostly given to the recycling of PS-probe and hence induced the Exo III-assisted signal amplification. Meanwhile, this technique was simple, easy-to-handle, and obtained the test results within 40 min. Furthermore, sensitive and rapid visualization determination can facilitate in-field and on-site applications without the assistance of instrumentation.

Selectivity To confirm the practical applicability of this colorimetric biosensor, the competition experiments and selectivity trials were conducted to evaluate the potential interferences

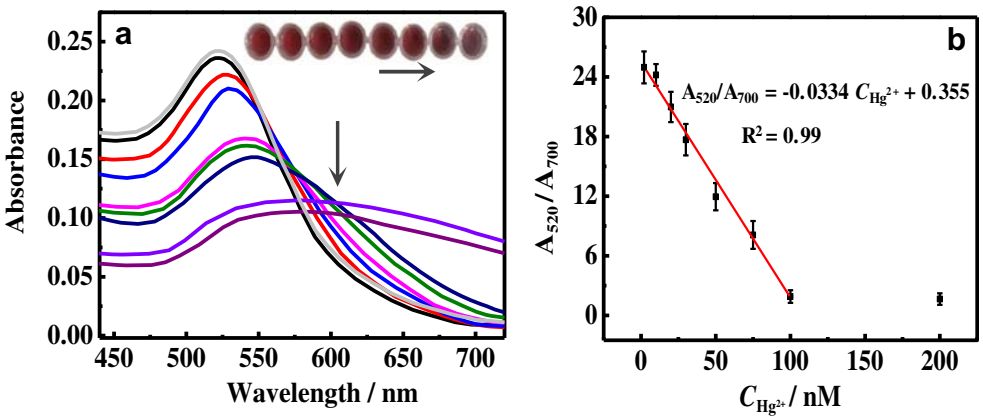

Fig. 3 **a** Visible spectra of the colorimetric biosensor under various amounts of Hg^{2+} in the order of curves top to bottom (curve 1–9): 0, 2, 10, 20, 30, 50, 75, 100, and 200 nM, Inset of the color display from left to right corresponds to the concentration of Hg^{2+} (0, 2, 10, 20, 30, 50, 75, and 100 nM) and **b** absorption ratio of A_{520}/A_{700} vs different Hg^{2+} concentration with linear fitting in the range of 2–100 nM

from potentially coexisting metal ions in water environments. Frequently encountered metal ions were chosen for the interference experiments under the optimal conditions same as for Hg^{2+} measurement. As illustrated in Fig. 4, only the presence of Hg^{2+} ions can result in a significant signal variation even though the interfering ions, including Mn^{2+}, Pb^{2+}, Ca^{2+}, Cd^{2+}, Cu^{2+}, Ni^{2+}, Fe^{2+}, Cr^{3+}, and Co^{2+}, existed at a high concentration in the samples.

Moreover, the colorimetric biosensor was further challenged with Hg^{2+} determination in the coexistence of interfering metal ions. Results showed that the coexistence of interfering metal ions posed a negligible impact on the performance of our protocol towards Hg^{2+}. These results further demonstrated the excellent selectivity of this sensing platform for Hg^{2+} determination even in the complicated matrixes. The selectivity was further confirmed by investigating the cleavage of the PS-probe incubated with 10 μM metal ions for 10 min. As unveiled by nondenaturing 15% PAGE image (Inset of Fig. 4), distinct bands with clearly different mobilities appeared only in the lanes contained Hg^{2+} ions, indicating the selective cleavage of the PS-probe caused by Hg^{2+} ions. This result accorded well with the absorption ratio described above.

Application in real water sample analysis To test the applicability of this biosensor for Hg^{2+} determination in real samples, two environmental water samples were taken from Guanting reservoir located in the north of Beijing, China, and tap water in lab. The colorimetric biosensor demonstrated a negligible signal change compared to the blank samples towards the raw water, suggesting no presence of Hg^{2+} or below the LOD of this method. Because the Hg^{2+} concentration of environment water was nondetectable, therefore the concentrations of 0, 5.0, and 10.0 nM of Hg^{2+} were spiked and analyzed, using this bioassay system and inductively coupled plasma mass spectrometry (ICP-MS), respectively. Each analysis was conducted in triplicate to minimize any possibilities of error. Therefore, a spike-recovery test was carried out by spiking Hg^{2+} ions at three concentration levels. The testing results of the biosensor towards the Hg^{2+}-spiked samples are demonstrated in Table S3. The quantitative recoveries in the range of 96–114% were achieved by using this method. The good accordance of measured values with the spiked Hg^{2+} concentrations suggested the prospective applicability of this method for Hg^{2+} determination in real water environments.

Conclusions

By incorporating a PS-probe and a recycled enzymatic cleavage to amplify the signal, we described a colorimetric

Table 1 Nanomaterial-based colorimetric sensors for the determination of Hg^{2+}

Materials used	Method	LOD	Reference
AuNPs	Hg^{2+} unfolds the arch-trigger duplex and induced aggregation of thymine-rich DNA modified AuNPs	3.4 nM	[27]
AuNPs	The functionalized gold nanoparticles with papain selectively response to Hg^{2+}	200 nM	[31]
AuNPs	The addition of amine-based chemical to promote the aggregation of Hg^{2+}-capped AuNPs	10 pM	[32]
AuNRs[1]	Hg^{2+} causes the disassembly of the modified AuNRs	5 nM	[33]
AgNPs[2]	The polydopamine adsorption with Hg^{2+} could induce the aggregation of AgNPs	30 nM	[34]
AuNPs	Hg^{2+} trigger the cleavage of the linker DNA, inhibiting the reformation of aggregated nanoparticle	1.30 nM	This study

[1] *AuNRs* gold nanorods, [2] *AgNPs* silver nanoparticles

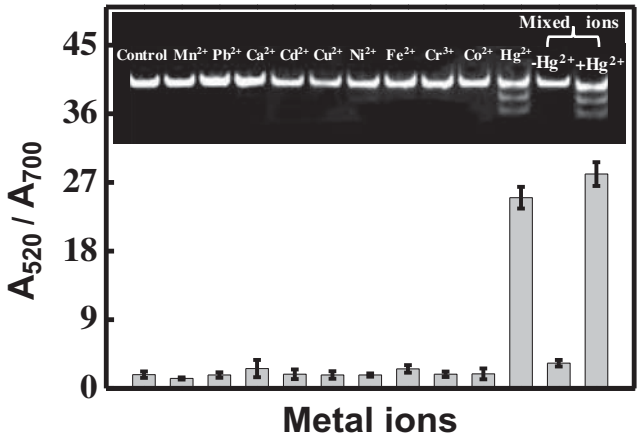

Fig. 4 Change of absorption ratio (A_{520}/A_{700}) for the colorimetric biosensor responding to different metal ions, e.g., Mn^{2+}, Pb^{2+}, Ca^{2+}, Cd^{2+}, Cu^{2+}, Ni^{2+}, Fe^{2+}, Cr^{3+}, Co^{2+}, and Hg^{2+}, and coexisting species as mentioned above in the absence and presence of Hg^{2+}. Inset: Nondenaturing 15% PAGE images exhibiting the cleavage of PS-probe incubated with 10 μM different metal ions for 10 min

biosensor for the rapid and sensitive determination of Hg^{2+} in water environments. This colorimetric biosensor obtained a LOD of 1.30 nM for Hg^{2+} determination. It exhibited an excellent selectivity for Hg^{2+} ions rather than other interfering metal ions even existed at high concentration. The applicability of this method was confirmed by results showing good recoveries (96–114%) in environmental water samples. In view of its simplicity, easy-to-handle, rapid, and sensitive visual determination, this biosensing method paves great potential for applications in on-site determination of Hg^{2+} without the aid of instrumentation for water pollution alarming and control. However, the cleavage yield of PS-probe that be further improved requires more research to in the future.

Funding information This research is supported by the Beijing Municipal Natural Science Foundation-Haidian Primitive Innovation Joint Fund Project (L182045).

Compliance with ethical standards

Conflict of interest The authors declare that they have no conflict of interest.

References

1. Jarup L (2003) Hazards of heavy metal contamination. Br Med Bull 68:167–182. https://doi.org/10.1093/bmb/ldg032
2. Zahir F, Rizwi SJ, Haq SK, Khan RH (2005) Low dose mercury toxicity and human health. Environ Toxicol Pharmacol 20(2):351–360. https://doi.org/10.1016/j.etap.2005.03.007
3. Li T, Dong S, Wang E (2009) Label-free colorimetric detection of aqueous mercury ion (Hg^{2+}) using Hg^{2+}-modulated G-quadruplex-based DNAzymes. Anal Chem 81(6):2144–2149. https://doi.org/10.1021/ac900188y
4. Nguyen VT, Kwon YS, Gu MB (2017) Aptamer-based environmental biosensors for small molecule contaminants. Curr Opin Biotechnol 45:15–23. https://doi.org/10.1016/j.copbio.2016.11.020
5. Kaur H, Bruno JG, Kumar A, Sharma TK (2018) Aptamers in the therapeutics and diagnostics pipelines. Theranostics 8(15):4016–4032. https://doi.org/10.7150/thno.25958
6. Zhang Y, Deng Y, Wang C, Li L, Xu L, Yu Y, Su X (2019) Probing and regulating the activity of cellular enzymes by using DNA tetrahedron nanostructures. Chem Sci 10(23):5959–5966. https://doi.org/10.1039/C9SC01912J
7. Ono A, Togashi H (2004) Highly selective oligonucleotide-based sensor for mercury(II) in aqueous solutions. Angew Chem Int Ed Engl 43(33):4300–4302. https://doi.org/10.1002/anie.200454172
8. Zhuang J, Fu L, Tang D, Xu M, Chen G, Yang H (2013) Target-induced structure-switching DNA hairpins for sensitive electrochemical monitoring of mercury (II). Biosens Bioelectron 39(1):315–319. https://doi.org/10.1016/j.bios.2012.07.015
9. Ling B, Ma Y, Chen H, Wang L (2017) A SPR aptamer sensor for mercury based on AuNPs@NaYF4:Yb,Tm,Gd upconversion luminescent nanoparticles. Anal Methods 9(42):6032–6037. https://doi.org/10.1039/C7AY01810J
10. Qi L, Zhao Y, Yuan H, Bai K, Zhao Y, Chen F, Dong Y, Wu Y (2012) Amplified fluorescence detection of mercury(II) ions (Hg^{2+}) using target-induced DNAzyme cascade with catalytic and molecular beacons. Analyst 137(12):2799–2805. https://doi.org/10.1039/C2AN35437C
11. Song X, Wang Y, Liu S, Zhang X, Wang H, Wang J, Huang J (2018) Ultrasensitive electrochemical detection of Hg^{2+} based on an Hg^{2+}-triggered exonuclease III-assisted target recycling strategy. Analyst 143(23):5771–5778. https://doi.org/10.1039/C8AN01409D
12. Huang PJ, van Ballegooie C, Liu J (2016) Hg^{2+} detection using a phosphorothioate RNA probe adsorbed on graphene oxide and a comparison with thymine-rich DNA. Analyst 141(12):3788–3793. https://doi.org/10.1039/C5AN02031J
13. Kiy MM, Jacobi ZE, Liu J (2012) Metal-induced specific and non-specific oligonucleotide folding studied by FRET and related biophysical and bioanalytical implications. Chemistry 18(4):1202–1208. https://doi.org/10.1002/chem.201102515
14. Kiy MM, Zaki A, Menhaj AB, Samadi A, Liu J (2012) Dissecting the effect of anions on Hg^{2+} detection using a FRET based DNA probe. Analyst 137(15):3535–3540. https://doi.org/10.1039/C2AN35314H
15. Hollenstein M, Hipolito C, Lam C, Dietrich D, Perrin DM (2008) A highly selective DNAzyme sensor for mercuric ions. Angew Chem Int Ed Engl 47(23):4346–4350. https://doi.org/10.1002/anie.200800960
16. Zhang XB, Kong RM, Lu Y (2011) Metal ion sensors based on DNAzymes and related DNA molecules. Annu Rev Anal Chem (Palo Alto, Calif) 4:105–128. https://doi.org/10.1146/annurev.anchem.111808.073617
17. Liu J, Lu Y (2007) Rational design of "turn-on" allosteric DNAzyme catalytic beacons for aqueous mercury ions with ultrahigh sensitivity and selectivity. Angew Chem Int Ed Engl 46(40):7587–7590. https://doi.org/10.1002/anie.200702006
18. Huang PJ, Wang F, Liu J (2015) Cleavable molecular beacon for Hg^{2+} detection based on phosphorothioate RNA modifications. Anal Chem 87(13):6890–6895. https://doi.org/10.1021/acs.analchem.5b01362
19. Rosi NL, Mirkin CA (2005) Nanostructures in biodiagnostics. Chem Rev 105(4):1547–1562. https://doi.org/10.1021/cr030067f
20. Borghei YS, Hosseini M, Dadmehr M, Hosseinkhani S, Ganjali MR, Sheikhnejad R (2016) Visual detection of cancer cells by colorimetric aptasensor based on aggregation of gold nanoparticles induced by DNA hybridization. Anal Chim Acta 904:92–97. https://doi.org/10.1016/j.aca.2015.11.026

21. Yang X, Xu J, Tang X, Liu H, Tian D (2010) A novel electrochemical DNAzyme sensor for the amplified detection of Pb^{2+} ions. Chem Commun (Camb) 46(18):3107–3109. https://doi.org/10.1016/j.aca.2015.11.026
22. Zhu D, Yan Y, Lei P, Shen B, Cheng W, Ju H, Ding S (2014) A novel electrochemical sensing strategy for rapid and ultrasensitive detection of Salmonella by rolling circle amplification and DNA-AuNPs probe. Anal Chim Acta 846:44–50. https://doi.org/10.1016/j.aca.2014.07.024
23. Turkevich J, Stevenson PC, Hillier J (1951) A study of the nucleation and growth processes in the synthesis of colloidal gold. Discussions of the Faraday Society 11:55–75. https://doi.org/10.1039/DF9511100055
24. Liu J, Lu Y (2004) Accelerated color change of gold nanoparticles assembled by DNAzymes for simple and fast colorimetric Pb^{2+} detection. J Am Chem Soc 126(39):12298–12305. https://doi.org/10.1021/ja046628h
25. Wang H, Liu Y, Liu G (2018) Electrochemical biosensor using DNA embedded phosphorothioate modified RNA for mercury ion determination. ACS Sens 3(3):624–631. https://doi.org/10.1021/acssensors.7b00892
26. Ye BC, Yin BC (2008) Highly sensitive detection of mercury (II) ions by fluorescence polarization enhanced by gold nanoparticles. Angew Chem Int Ed 47(44):8386–8389. https://doi.org/10.1002/anie.200803069
27. Liu S, Leng XQ, Wang X, Pei QQ, Cui XJ, Wang Y, Huang JD (2017) Enzyme-free colorimetric assay for mercury (II) using DNA conjugated to gold nanoparticles and strand displacement amplification. Microchim Acta 7(184):1969–1976. https://doi.org/10.1007/s00604-017-2182-7
28. Geng Z, Zhang H, Xiong Q, Zhang Y, Zhao H, Wang G (2015) A fluorescent chitosan hydrogel detection platform for the sensitive and selective determination of trace mercury (II) in water. J Mater Chem A 3(38):19455–19460. https://doi.org/10.1039/C5TA05610A
29. Elghanian R, Storhoff JJ, Mucic RC, Letsinger RL, Mirkin CA (1997) Selective colorimetric detection of polynucleotides based on the distance-dependent optical properties of gold nanoparticles. Science 277(5329):1078–1081. https://doi.org/10.1126/science.277.5329.1078
30. Li L, Li B, Qi Y, Jin Y (2009) Label-free aptamer-based colorimetric detection of mercury ions in aqueous media using unmodified gold nanoparticles as colorimetric probe. Anal Bioanal Chem 393(8):2051–2057. https://doi.org/10.1007/s00216-009-2640-0
31. Guo YM, Wang Z, Qu WS, Shao HW, Jiang XY (2011) Colorimetric detection of mercury, lead and copper ions simultaneously using protein-functionalized gold nanoparticles. Biosens Bioelectron 26(10):4064–4069. https://doi.org/10.1016/j.bios.2011.03.033
32. Chen YJ, Yao L, Deng Y, Pan DD, Ogabiela E, Cao JX, Adeloju SB, Chen W (2015) Rapid and ultrasensitive colorimetric detection of mercury (II) by chemically initiated aggregation of gold nanoparticles. Microchim Acta 182(13–14):2147–2154. https://doi.org/10.1007/s00604-015-1538-0
33. Liang GX, Wang L, Zhang HQ, Han ZX, Wu XX (2012) A colorimetric probe for the rapid and selective determination of mercury (II) based on the disassembly of gold nanorods. Microchim Acta 179:345–350. https://doi.org/10.1007/s00604-012-0882-6
34. Li K, Liang AH, Jiang CN, Li F, Liu QG, Jiang ZL (2012) A stable and reproducible nanosilver-aggregation-4-mercaptopyridine surface-enhanced Raman scattering probe for rapid determination of trace Hg^{2+}. Talanta 99:890–896. https://doi.org/10.1016/j.talanta.2012.07.052